Iran J Public Health, Vol. 51, No.9, Sep 2022, pp.2048-2059

Original Article

Compound Homozygous Rare Mutations in PLCE1 and HPS1 Genes Associated with Autosomal Recessive Retinitis Pigmentosa in Pakistani Families

Masroor Ellahi Babar [1], Akhtar Ali [2], Syed Hassan Abbas [3], Mirza Jawad Ul Hasnain [3], Nida Babar [4], Hira Babar [5], Tanveer Hussain [6], Asif Nadeem [6], Namra Ayub [2], Sundus Shahid [2], *Muhammad Tariq Pervez [3]

1. *The University of Agriculture, Dera Ismail Khan, Pakistan*
2. *Department of Biotechnology, Virtual University of Pakistan, Lahore, Pakistan*
3. *Department of Bioinformatics & Computational Biology, Virtual University of Pakistan, Lahore, Pakistan*
4. *Resident Histopathology, Shaukat Khanum Memorial Hospital, Lahore, Pakistan*
5. *Resident Hematology, Mayo Hospital, Lahore, Pakistan*
6. *Department of Molecular Biology, Virtual University of Pakistan, Lahore, Pakistan*

***Corresponding Author:** Email: m.tariq@vu.edu.pk

(Received 19 Apr 2021; accepted 09 Jun 2021)

Abstract

Background: Retinitis pigmentosa (RP) belongs to pigmentary retinopathies, a generic name for all retinal dystrophies with a major phenotypical and genotypical variation, characterized by progressive reduction of photoreceptor functionality of the rod and cone. Global prevalence of RP is ~ 1/4000 and it can be inherited as autosomal dominant (adRP), autosomal recessive (arRP) or X- linked (xlRP). We designed this study to identify causative mutations in Pakistani families affected with arRP.

Methods: In 2019, we recruited two unrelated Pakistani consanguineous families affected with progressive vision loss and night blindness from Punjab region. Clinical diagnosis confirmed the; bone spicule pigmentation of the retina, and an altered electroretinogram (EGR) response. Proband and healthy individual from each family were subjected for whole-exome sequencing (WES). Various computational tools were used to analyze the Next Generation Sequencing (NGS) data and to predict the pathogenicity of the identified mutations.

Results: WES data analysis highlighted two missense homozygous variants at position c.T1405A (p.S469T) in *PLCE1* and c.T11C (p.V4A) in *HPS1* genes in proband of both families. Healthy individuals of two families were tested negative for p.S469T and p.V4A mutations. The variant analysis study including molecular dynamic simulations predicted mutations as disease causing.

Conclusion: Compound effect of mutations in rarely linked *PLCE1* and *HPS1* genes could also cause RP. This study highlights the potential application of WES for a rapid and precise molecular diagnosis for heterogeneous genetic diseases such as RP.

Keywords: Retinitis pigmentosa; Whole-exome sequencing; Pakistan

Introduction

Retinitis pigmentosa (RP: MIM26800) belongs to pigmentary retinopathies, a generic name for all retinal dystrophies with a major phenotypical and genotypical variation, characterized by progressive reduction of photoreceptor functionality of the rod and cone (1). Approximately, 1.5 million people worldwide lose eye sight every year due to retinal degeneration (2). The disease is a particularly heterogeneous with a global prevalence of ~ 1/4000 and it can be inherited as autosomal dominant RP (adRP), autosomal recessive (arRP) or X- linked (xlRP) (3). The first symptoms of RP, often noted in adolescence, are night vision disturbances and loss of the mid peripheral visual field. Secondary, the loss of cone photoreceptors may result in central vision deficiency and, eventually, leads to legal blindness. In advance stage of disease, the retinal vessels are attenuated, and the optic nerve head appears pale and waxy (4,5). Over recent years, tremendous efforts have been made in research leadings to an early detection of retinal degeneration.

Surprisingly, the great success of discovering RP-causing genes and mutations over the past two decades has revealed the extent of the uncertainty and complexity. On the other hand, being a molecular level disease, rather than a clinical level, its treatment is comparatively easy. At present, according to the RetinoGenetics database (http://www.retinogenetics.org/) more than 66 genes have been identified with non-syndromic RP. Several approaches are being used to classify genes and the underlying mutations. Majority of genes were identified by sequencing the candidates' genes in selected patient populations. A retina gene may be a candidate for the disease due to its functional properties, or it is identical with a gene known to cause retinal disease, or because it is the cause of retinal disease in animal model (6). Most cases were observed due to mutations within a single gene. Now a days, whole-exome sequencing (WES) has been proven the most effective tool to identify autosomal recessive RP (arRP) genes and mutations.

Due to the relatively high level of consanguinity, large number of siblings in families and the presence of isolated subpopulations, family based gene analysis is highly effective in sub-continent population (7). This study presents WES analysis of RP patients (Pakistani families) to identify causative mutations(s). In additions, this study also deals with the MD simulations prediction and the fate of causative mutations in the target domain.

Materials and Methods

Subjects

The study protocol was approved by the Ethical Committee of Virtual University of Pakistan (Ethical#2019/A1021) and adhered with the principle of the declaration of Helsinki.

We recruited two consanguineous families after obtaining a written consent. Pedigrees were drawn and patients were diagnosed clinically by an ophthalmologist. RP patients were diagnosed with progressive vision loss, night blindness, overall bone spicule pigmentation of the retina, and an altered electroretinogram (EGR) response. Blood samples were collected for molecular analysis. One proband diagnosed with RP, one phenotypically unaffected member from each family was selected for whole-exome sequencing (WES). The pedigree was drawn according to detailed interview with affected families as shown in Fig. 1A & 1B.

Genomic DNA Isolation

Approximately 3 mL peripheral blood samples were collected from the recruited participants for genomic DNA extraction. Whole DNA was extracted using GeneJET genomic DNA purification kit (CAT # K0721) according to the manufacturer's protocol. The extracted DNA was quantified with NanoDrop spectrophotometer (Thermo Scientific, US). The DNA was stored at -20 ºC for further use.

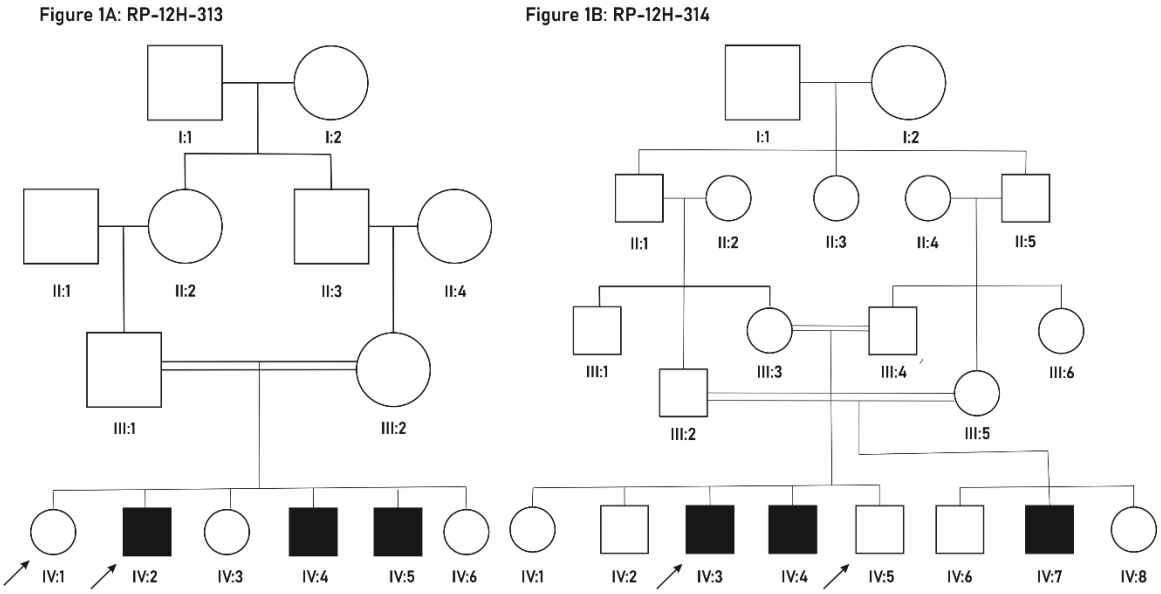

Fig. 1: Pedigrees of Pakistani families RP-12H-313 and RP-12H-314, (A) Arrow indicates the proband IV:2 in family RP-12H-313. (B) Arrow indicates the proband IV:3 in family RP-12H-314, solid symbol indicates affected individual and open symbols indicate unaffected individuals

Library Preparation and Whole-exome Sequencing

In the process, 3 µg of pure and high molecular weight genomic DNA was used for exome libraries preparation. Target enrichment was performed to construct the exome-library using the Agilent Sure-Select all exon Ver5 kit (Agilent Technologies, Inc. Santa Clara, CA, US) according to the manufacturer's instructions, which targets 50Mb of the exonic regions of human genome. QIAxcel Advanced System (Qiagen, Hilden, Germany) was used for libraries validation and Qubit Fluoremeter (Thermo Fisher scientific) was used for libraries quantification. Whole-exome paired end sequencing for the affected individual and a healthy family member was performed with average read length of 100 bp using Illumina HiSeq 2000 platform (Illumina, Inc. San Diego, CA, United State) according to the manufacturer's instructions. Exome sequencing was performed commercially at the BGI Tech Solutions Co., Ltd. (Hong Kong, China).

Whole-exome Sequencing (WES) Data analysis

Quality of reads was assessed using FastQC. High-quality sequencing reads were mapped with BWA - Burrows-Wheeler Alignment tool to human reference genome (GRCh37.p13/hg19 – Genome Reference Consortium Human Build 37 patch release 13 - NCBI) (8). Sequences marked as PCR duplicates were discarded from the BAM file by using Picard tool (https://broadinstitute.github.io/picard/).

SAMtools and GATK (Genome Analysis Toolkit) were applied for the variants calling process (9,10). High-quality variants were filtered as follows; (a) Base-quality ≥ 30 (b) Depth ≥ 10. ANNOVAR was used for annotation of variants and further downstream analysis (11). For prioritization of variants three majors steps were taken; (a) excluded intronic and synonymous SNVs (b) Variants were filtered and selected on the basis of frequency (AF < 5% in 1000 Genomes Project Database, Genome Aggregation Database (gnomAD) and National Heart, Lung and Blood Institute (NHLBI) Exome Sequencing Project Da-

tabase; (c) Six different tools SIFT, PolyPhen-2, LRT, MutationTaster, MutationAssessor and PROVEAN were used for predicting the functional effects of variants (12–16). Further, Genomic Evolutionary Rate Profiling ++ (GERP) Rejected Substitution has estimated the sequence conservation of candidate variants (17).

Mutation Validation

After read calling and filtration against multiple databases, genomic variants were identified. Validation of the mutations in patients was performed by comparison of WES of un-affected members of RP-12H-313 and RP-12H-314 families.

Protein Modeling and Molecular dynamic simulations

As previously, no protein structure of identified causative gene was reported, so for 3-D structure prediction MODELLER 9.23 was used (18). The protein sequence of amino acids was downloaded from UniProtKB (Q92902) and then model prediction was repaired and normalized the structure using FOLDX 5.0 (19). PyMol 2.2 was used to induce mutation in the native protein structure. After the structure evaluation using ERRAT, we performed molecular dynamic simulation of both native and mutant structure by using GROMACS 5.0 (20). Systems were first minimized and equilibrated in NaCl and simulated at 30ns MD at a temperature of 300K under 1 atm pressure. g_rmsd, g_rmsf, g_gyrat, g_hbond tools were used to study the structural behaviors of native and mutant protein. Solvent accessibility of amino acid residues was determined using g_sasa tool to see the effect of mutation in the normal protein structure and the impact of mutation at hydrogen bonding residues.

Results

In order to identify causative variants associated with disease course, proband and one healthy individual from both Retinitis Pigmentosa (RP) families were recruited Fig.1. Both RP patients were presented with progressive vision loss, night blindness, overall bone spicule pigmentation of the retina, and an altered electroretinogram (EGR) response. The fundus examination of patient IV:2 in RP-12H-313 family shown in Fig.2. A flowchart summarizing the main steps of the study including design and analysis is depicted in Fig.3.

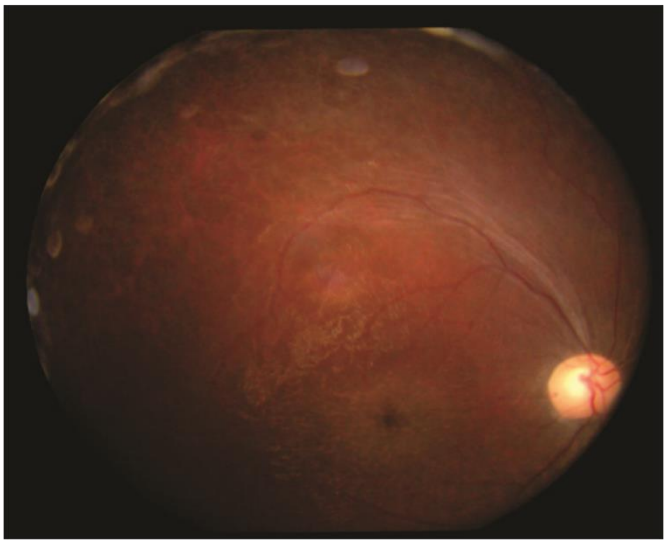

Fig. 2: Fundus examination of right eye Patient IV:2 in family RP-12H-313, showed typical signs of RP; pigment formation

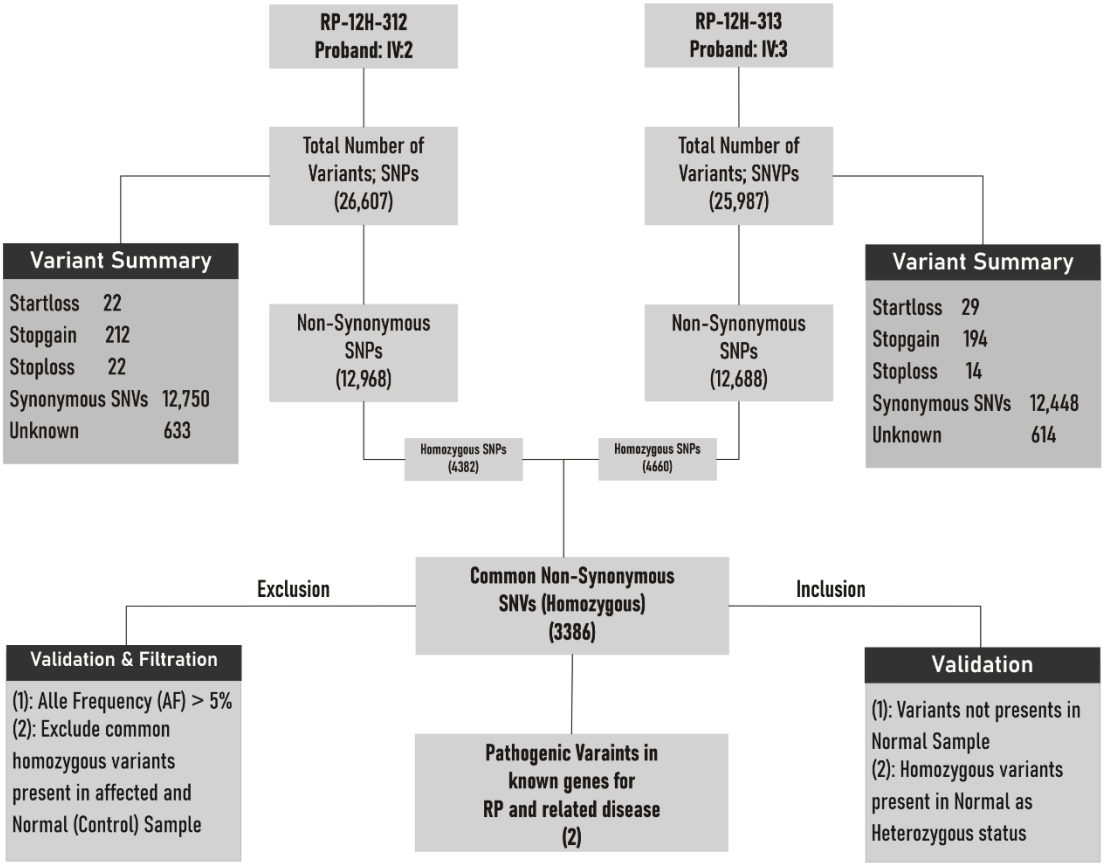

Fig. 3: Systematic workflow summarizing the main steps of the study design and analysis

Whole-exome sequencing data analysis (Landscape of identified RP associated genes mutations)

To identify genomic mutations in disease-causing genes associated with RP, we considered whole-exome sequencing (WES), a typical capture array-based method of Next Generation Sequencing (NGS), applied to all exomic data at 100x coverage. The WES of Proband IV:2 (RP-12H-313 family), Proband IV:3 (RP-12H-314 family), generated 45.42 and 48.12 millions bases of sequence with 100x coverage respectively. The 26,607 functional SNPs that may affect amino acid sequence were identified in proband IV:2 of family RP-12H-313 and 25,987 SNPs that also affect amino acid sequence were identified in proband IV:3 of family RP-12H-314 (Table 1). Moreover, the maximum depth coverage was 98%, enough to reliably identify variants within majority of the exome regions in the genomic DNA. Complete variants distribution and workflow of whole-exome sequencing analysis are shown in Fig.3. The results of associated genes were also compared with the previous whole-genome and whole-exome sequencing results accessible from the SNPs reference databases such as dpSNP, Ensemble. According to the established criteria, by excluding the heterozygous variants and synonymous mutations, we identified two rare mutations in *PLCE1* (exon3:c.T1405A:p.S469T) and *HPS1* (exon3:c.T11C:p.V4A) genes in each proband of both families as shown in Table 2.

Table 1: Summary of variations, Candidates SNPs filtered against several public variation databases

Variable	*Feature – SNPS in patient IV:2 of family RP-12H-313*	*Feature – SNPS in patient IV:3 of family RP-12H-314*
Total number of variations (SNPs)	26,607	25,987
Total Number of non-synonymous SNPs	12,968	12,688
Total Number of synonymous SNPs	12,750	12,448
Variations with unknown functionality	633	614
Homozygous SNPs	4382	4660
Common non-synonymous homozygous SNPs	3386	
Filtered Causative variants	2	

Table 2: Identified Variants by whole exome sequencing analysis in combination with Retinitis pigmentosa (RP) gene filters in the families RP-12H-313 and RP-12H314

Chr	*Position (bp (hg19))*	*Reference Allele*	*Mutant Allele*	*Reference Amino Acid*	*Mutant Amino Acid*	*Gene*	*Functional Prediction*[a]	*GERP ++ RS*[b]	*1000G_ALL_AF*	*ESP6500si_ALL*	*gnomAD_ALL*
10	95892129	T	A	S	T (p.S469T)	PLCE1	D,P,B,N,N,N,N	4.84	0.017	0.03	0.031
10	100202987	A	G	V	A (p.V4A)	HPS1	D,D,P,D,D,M,D	4.62	0.041	0.035	0.0313

[a]Funtional effects predicted by SIFT, PolyPhen-2_HDIV, PolyPhen-2_HVAR, LRT, MutationTaster, MutationAssessor and PROVEAN in order. Deleterious effect was denoted as D, Probably Damaging as P, Benign as B, M as Medium, and N as Neutral

[b]Genomic Evolutionary Rate Profiling ++ Rejected Substitution score (The larger the score, the more conserved site)

Abbreviations: Chr, chromosome; All, all populations; AF, allele frequency; 1000G, 1000 Genomes Project; ESP6500si, NHLBI Go Exome Sequencing Project (ESP) – Exome Variants Server; gnomAD, The Genome Aggregation Database

Causative mutation validation and analysis

The WES data of one phenotypically healthy individual from each family was also analyzed and both the normal individual were tested negative for p.S469T and p.V4A in *PLCE1* and *HPS1* respectively. These finding revealed that both mutations have significant association with RP disease development in two Pakistani families.

Functional and structural analysis by MD simulations

We further studied that whether the mutation in *HPS1* gene alters the translated regions of *HPS1* protein and change the protein structural behavior or not. For this purpose, we first predicted the tertiary structure of *HPS1* protein (Fig.4) and then indicated the beta sheet where V4A mutation altered the structure in Fig.4B & 4C. The predicted protein structure had A chain contains 18 Alpha helices (41.57% of total sequence), 19 beta sheets (14 % of total sequence) and 34 coils (44.43% of the total sequence) shown in Fig.4D.

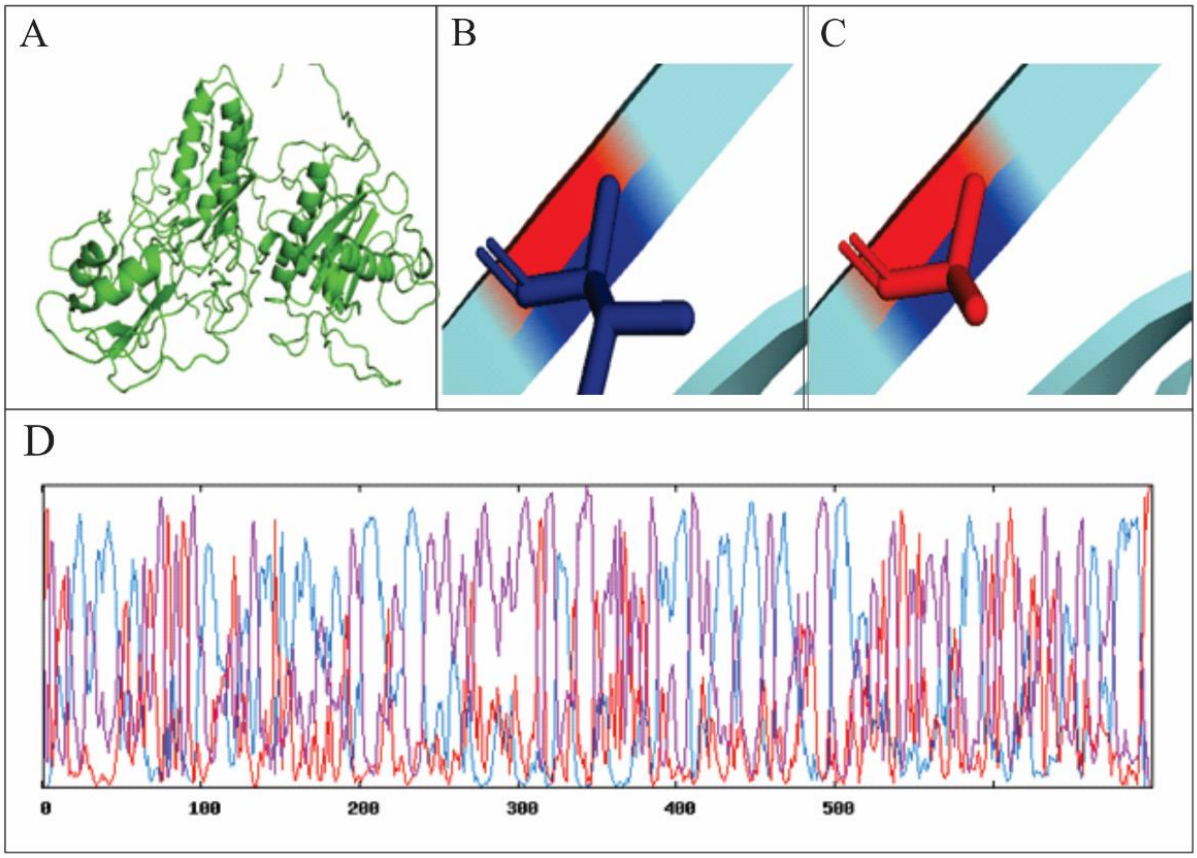

Fig.4: A) 3-D structure of HPS1 protein (B &C) Mutation at point V4A D) Secondary Structure of Protein HPS1

The mutation V4A was situated at beta sheet which is outside of the transmembrane. After the energy minimization of both native and mutant *HPS1* protein structures, we equilibrated the structures and thermostat (NVT) and bariostat (NPT) equilibration were performed to set the nest orientation pf all molecules present in our structures. Density, pressure and temperature graphs were established using gms_grompp tool. Fig.5A showed the density plot of both wild and mutant structures of *HPS1* protein structures at 1000 kgm^{-3} over the time of 100 ps. Plot showed the average density of all conformations of native structure was 1001.261 kgm^{-3} which is rarely close to the actual experimental value of 1000kgm^{-3} while that of the mutant V4A protein structure was 1002.141 kgm^{-3} which showed much fluctuation as compared to the normal protein. Pressure plot (Fig.5B) depicted the fluctuation of residues conformations over the time ranging from -125 bars to 137 bars with an average of -2.4 bars. Mutant structure showed pressure plot over the time of 100 ps ranging from -102 bars to 85 bars with an average of -1.16 bars. Temperature plot (Fig.5C) showed that all the conformations of native protein residues fluctuated ranging from 298.37 K to 301.22 with an average of 300.01 K. while that of the mutant structure was ranging from 396.72 K to 301.32 K with an average of 299.97 K.

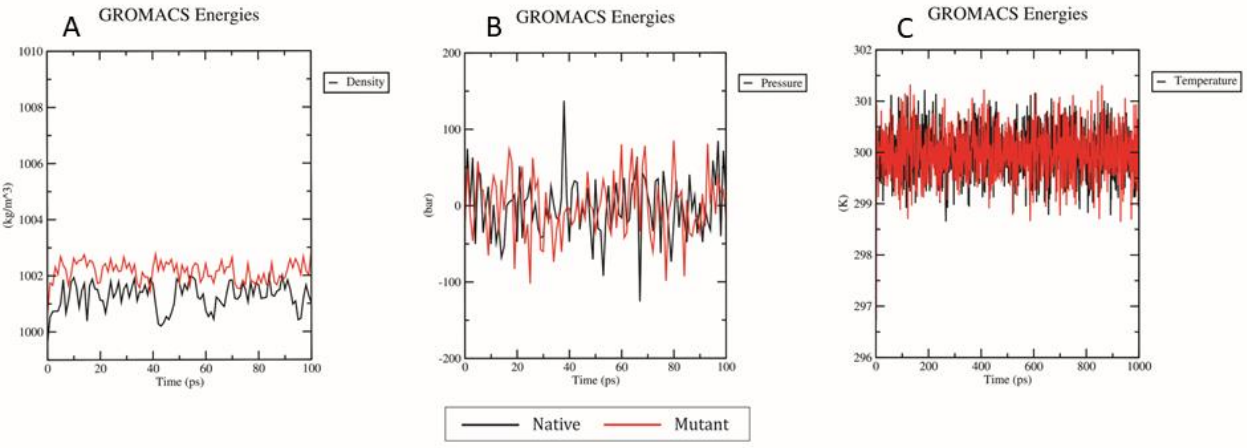

Fig. 5: Density (A), Pressure (B) and Temperature (C) versus time graphs of native and mutant HPS1 protein. Native graph is shown in black and mutant graph is shown in red color

After the equilibration of both systems, root mean square deviation and root mean square fluctuation of both structures were evaluated to observe the structural variations in native *HPS1* and its mutant. Fig.6A showed the rmsd of both native and mutant where plot showed that the overall fluctuation of native model ranged from 0.00498 nm to 0.719039 nm with an average of 0.590577 nm. The peak of the graph was found at around 12.54 ns whereas the minimum value was recorded in the very start of the graph. Over the course of last 10 ns, we found a streamlined fluctuation near to the average. Rmsd value of mutant on the other hand showed a great fluctuation for each conformation over the time with a maximum value of 1.515 nm attained at 24.3 ns and a least value of 0.0004975 nm at zero ns. The average rmsd value of mutant structure was 1.41 ns which was far high from the average value of native structure. Rmsf value of both structures (Fig.6B) showed that net fluctuation of mutant structure is quite higher than that of the native with an effective difference of around 0.21 nm.

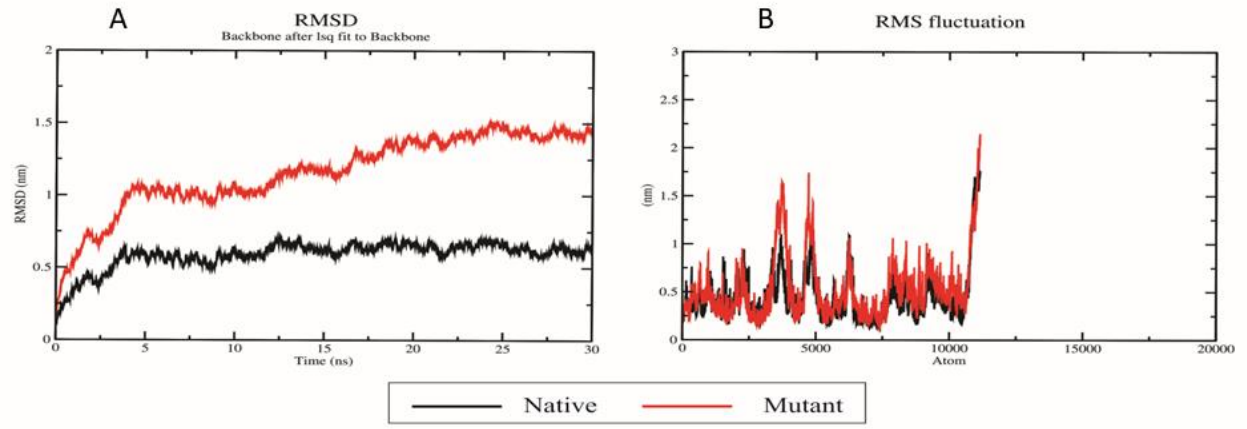

Fig. 6: RMSD (A) and RMSF (B) versus time graphs of native and mutant HPS1 protein. Native graph is shown in black and mutant graph is shown in red color

It was notable that rmsf of mutant structure reached up to 2.2 nm in the end and 1.75 nm at 4.8 ns which was higher than the maximum peak of the rmsf values of the native structure. Solvent

accessibility of surface area (SASA) is defined as the surface area of any biomolecule which is directly accessible to the water of the system`s box. An increase in SASA means that protein is more stable and exposed while a decrease in SASA value indicates that the biomolecule is shrunken, buried and less stable. Native and mutant protein structures (Fig.7A) showed a great variation where in the start, SASA value of native structure was 540 nm^2 whereas mutant structure had initial value at 531 nm^2. Average SASA value of native structure is 453 nm^2 whereas that of the mutant structure had 450 nm^2.

Radius of gyration (Rg) is defined as radius of a protein structure about an axis of rotations. It usually calculates the RMS distance of all atoms from their common axis of rotation on the basis of mass-weight. Higher the Rg means lowers the stability of protein whereas lower the Rg means the structure is more stable. Rg of native structure ranged from 3.75 to 3.195 nm with an average of 3.35 nm while the mutant structure had the range between 3.725 to 3.16 nm with an average of 3.28 nm (Fig.7B). Fig.7C showed that number of hydrogen bonds got reduced over the course of time for mutant structure as compared to the native structure of *HPS1* protein. A clear difference of 27-30 hydrogen bonds was seen after 7 ns.

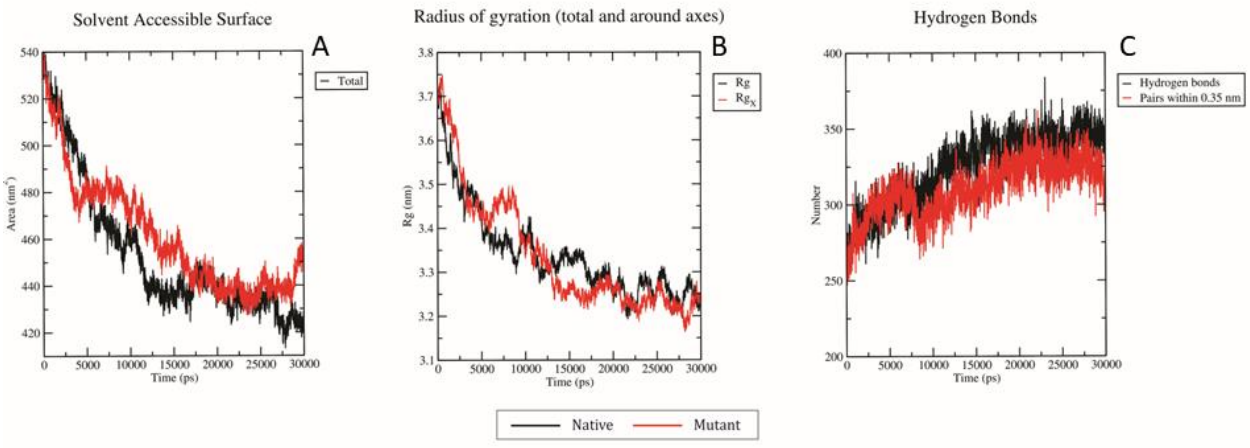

Fig. 7: SASA (A), Radius of gyration (B) and Hydrogen Bonds in model (C) versus time graphs of native and mutant HPS1 protein. Native graph is shown in black and mutant graph is shown in red color

Discussion

Retinitis pigmentosa (RP) is a heterogenous, progressive degenerative disease leading to profound vision loss or blindness (21). Mutational analysis of heterogenous disorder through next generation sequencing has been proved very helpful (22). We performed whole exome sequencing analysis of probands of two different RP families with autosomal recessive inheritance pattern.

We identified two rare causative mutations c.T1405A (p.S469T) in PLCE1 and c.T11C (p.V4A) in *HPS1* gene. Clinical investigation of retina correlates both families with arRP. Members of each family without clinical sign and symptoms were tested negative for p.S469T and p.V4A mutations in PLCE1 and HSP1genes respectively. Both mutations were predicted to be disease causing by SIFT, PolyPhen-2, LRT, MutationTaster, MutationAssessor and PROVEAN. Furthermore, molecular dynamic simulation analysis predicted p.V4A in *HPS1* gene as a pathogenic variant.

Phospholipase C epcilon 1 gene (OMIM:608414) encodes phospholipase which catalyzes the hydrolysis of phosphatidyl biphosphate and generates inositol 1,4,5 triphosphate (IP3) and diacyl glycerol (DAG). IP3 is required for intracellular Ca^{2+} release via IP3 receptors

(23). The subsequent products regulate various cellular growth, differentiation and expression processes. Expression of PLCE1 correlates with neural differentiation of stem cell and malfunctioning leads to retinodystrophy (24). PLCE1 is a bifunctional enzyme it also regulates small GTPases of ras superfamily through guanine-echange factor (RasGEF). Small GTPases are involved in embryonic differentiation and postnatal development of retina. Mutations in has been described associated with onset nephrotic syndrome, diffuse mesengial sclerosis and focal segmental glomerulosclrerosis. Our WES data suggest that truncated mutation at p.S469T in PLCE1gene could also lead to autosomal recessive retinitis pigmentosa (arRP).

Hermansky-Pudlak syndrome 1 (HPS1) gene located at 10q24 position transcribes a novel transmemberane protein, an important component of biogenesis of lysosomal organelles complex 3 (BLOC3) found in melanosomes, platelet-dense granules organelles and lysosomes (25). Melanosomes synthesize and store melanin pigment in retinal epithelial cells. Mutations in HSP1 gene results in morphological abnormalities in melanosomes (26). In this study, p.V4A in *HPS1* gene found in affected members of two different consanguineous families. In addition to other *in-silico* tools, molecular dynamic (MD) simulation also predicted it as pathogenic. MD modeling is helpful to predict single base change impact on protein structure (16). Molecular dynamics predicted that V4A mutation alters the beta sheet of tertiary structure of *HPS1* protein (Fig. 4A, 4B & 4C). The predicted protein structure had A chain contains 18 Alpha helices (41.57% of total sequence), 19 beta sheets (14 % of total sequence) and 34 coils (44.43% of the total sequence) shown in Fig.4D.

NGS technique has made a great contribution in molecular genetic data. RP studies have attained significant attention in the recent decades. To-date more than 66 genes associated with non-syndromic RP has been reported as listed on RetinoGenetics (http://www.retinogenetics.org/).

About 30% of total reported mutations are prevalent in *RHO, USH2A* and *RPGR* genes. Ethnic variations, a set of responsible genes and highly heterogeneous nature of RP indicates that mutations in one population may not be the common in other groups (27). Available data depicts that casual mutations in PLCE1 and HSP1 gene account very less for development of RP. PLCE1 protein is an important enzyme which indirectly regulates the retinal development. Similarly, HSP1 is responsible for retinal pigment storage and synthesis. Our data revealed that two rare mutations in *PLCE1* and *HSP1* genes in two unrelated Pakistani families have pathogenic affect.

Conclusion

Identified two pathogenic mutations p.S469T in PLCE1 and p.V4A in *HPS1* genes are associated with arRP. Exome sequence data filtration, computational prediction and molecular dynamic analysis can serve as a reference to evaluate the association of causative mutations. Prevalence of two mutations in unrelated RP families indicates the potential synergistic effect of PLCE1 and HSP1 molecules in RP development. This data could be a valuable source for future investigations to explore the combined effect of multiple mutations in genetic diseases.

Journalism Ethics considerations

Ethical issues (Including plagiarism, informed consent, misconduct, data fabrication and/or falsification, double publication and/or submission, redundancy, etc.) have been completely observed by the authors.

Acknowledgements

Authors appreciate the contribution of affected family members in accomplishment of this study. Virtual University of Pakistan is acknowledged for financial support in conducting this study.

Conflict of interest

The authors declare that there is no conflict of interests.

References

1. Dias M, Joo K, Kemp J, et al (2018). Molecular genetics and emerging therapies for retinitis pigmentosa: Basic research and clinical perspectives. *Prog Retin Eye Res,* 63:107-131.
2. Estrada-Cuzcano A, Neveling K, Kohl S, et al (2012). Mutations in C8orf37, encoding a ciliary protein, are associated with autosomal-recessive retinal dystrophies with early macular involvement. *Am J Hum Genet*, 90 (1):102–9.
3. Bovolenta P, Cisneros E (2009). Retinitis pigmentosa: cone photoreceptors starving to death. *Nat Neurosci,* 12(1):5–6.
4. Altintas N, Sarica Yilmaz Ö, Soylu A, Biçer I (2017). Analysis of mutations of Retinitis pigmentosa by sequencing. *J Appl Biol Sci,* 11(1):11–4.
5. Sumaroka A, Cideciyan A V, Charng J, et al (2019). Autosomal Dominant Retinitis Pigmentosa Due to Class B Rhodopsin Mutations: An Objective Outcome for Future Treatment Trials. *Int J Mol Sci*, 20(21):5344.
6. Picaud S, Dalkara D, Marazova K, Goureau O, Roska B, Sahel J-A (2019). The primate model for understanding and restoring vision. *Proc Natl Acad Sci U S A*, 116(52):26280–7.
7. Naibkhil N, Chitkara E (2016). Consanguineous marriages increase risk of congenital anomalies-studies in four generation of an afghan family. *Biomed Res,* 27(1):34–9.
8. Li H, Durbin R (2010). Fast and accurate long-read alignment with Burrows-Wheeler transform. *Bioinformatics,* 26(5):589–95.
9. Van der Auwera GA, Carneiro MO, Hartl C, et al (2013). From fastQ data to high-confidence variant calls: The genome analysis toolkit best practices pipeline. *Curr Protoc Bioinformatics,* 43(1110):11.10.1-11.10.33.
10. Li H, Handsaker B, Wysoker A, et al (2009). The Sequence Alignment/Map format and SAMtools. *Bioinformatics,* 25(16):2078–9.
11. Wang K, Li M, Hakonarson H (2010). ANNOVAR: Functional annotation of genetic variants from high-throughput sequencing data. *Nucleic Acids Res,* 38(16):e164.
12. Clarke L, Zheng-Bradley X, Smith R, et al (2012). The 1000 Genomes Pproject: Data management and community access. *Nat Methods,* 9(5):459-62.
13. Ng PC, Henikoff S (2003). SIFT: Predicting amino acid changes that affect protein function. *Nucleic Acids Res,* 31(13):3812–4.
14. Clemens DJ, Lentino AR, Kapplinger JD, et al (2018). Using the genome aggregation database, computational pathogenicity prediction tools, and patch clamp heterologous expression studies to demote previously published long QT syndrome type 1 mutations from pathogenic to benign. *Heart Rhythm,* 15(4):555–61.
15. Choi Y, Sims GE, Murphy S, Miller JR, Chan AP (2012). Predicting the Functional Effect of Amino Acid Substitutions and Indels. *PLoS One,* 7(10):e46688.
16. Hasnain MJU, Shoaib M, Qadri S, et al (2020). Computational analysis of functional single nucleotide polymorphisms associated with SLC26A4 gene. *PLoS One,* 15(1):e0225368.
17. Huber CD, Kim BY, Lohmueller KE (2020). Population genetic models of GERP scores suggest pervasive turnover of constrained sites across mammalian evolution. *PLoS Genet,* 16(5):e1008827.
18. Eswar N, Webb B, Marti-Renom MA, et al (2006). Comparative protein structure modeling using Modeller. *Curr Protoc Bioinformatics,* Chapter 5:Unit-5.6.
19. Schymkowitz J, Borg J, Stricher F, et al (2005). The FoldX web server: an online force field. *Nucleic Acids Res,* 33: W382–8.
20. Abraham MJ, Murtola T, Schulz R, et al (2015). GROMACS: High performance molecular simulations through multi-level parallelism from laptops to supercomputers. *SoftwareX,* 1–2:19–25.
21. Fernandez-San Jose P, Corton M, Blanco-Kelly F, et al (2015). Targeted Next-Generation Sequencing Improves the Diagnosis of Autosomal Dominant Retinitis Pigmentosa in Spanish Patients. *Invest Ophthalmol Vis Sci,* 56(4):2173–82.
22. Ávila-Fernández A, Cantalapiedra D, Aller E, et al (2010). Mutation analysis of 272 Spanish

families affected by autosomal recessive retinitis pigmentosa using a genotyping microarray. *Mol Vis*, 16:2550–8.

23. Schmidt M, Evellin S, Weernink PAO, et al (2001). A new phospholipase-C-calcium signalling pathway mediated by cyclic AMP and a Rap GTPase. *Nat Cell Biol*, 3(11):1020–4.
24. Zhang CL, Zou Y, Yu RT, Gage FH, Evans RM (2006). Nuclear receptor TLX prevents retinal dystrophy and recruits the corepressor atrophin1. *Genes Dev*, 20(10):1308–20.
25. Nazarian R, Falcón-Pérez JM, Dell'Angelica EC (2003). Biogenesis of lysosome-related organelles complex 3 (BLOC-3): A complex containing the Hermansky-Pudlak syndrome (HPS) proteins HPS1 and HPS4. *Proc Natl Acad Sci U S A,* 100(15):8770–5.
26. Sarangarajan R, Budev A, Zhao Y, Boissy RE, Gahl WA (2001). Abnormal Translocation of Tyrosinase and Tyrosinase-Related Protein 1 in Cutaneous Melanocytes of Hermansky–Pudlak Syndrome and in Melanoma Cells Transfected with Anti-Sense HPS1 cDNA. *J Invest Dermatol,* 117(3):641–6.
27. Ali MU, Rahman MSU, Cao J, Yuan PX (2017). Genetic characterization and disease mechanism of retinitis pigmentosa; current scenario. *3 Biotech,* 7(4):251.